

Diabetes Intervention Trial (J-EDIT). Diabetes/Metabolism Research and Reviews, in press

51) Oizumi XS, Akisaki T, Kouta Y, Song XZ, Takata T, Kondoh T, Umetani K, Hirano M, Yamasaki K, Kohmura E, Yokono K, Sakurai T: Impaired response of perforating arteries to hypercapnia in chronic hyperglycemia. Kobe Journal of Medical Science, in press

52) Song XZ, Wu B, Takata T, Wang XN, Oizumi XS, Akisaki T, Yokono K, Sakurai T: Neuroprotective Effect of D-Fructose-1,6-Bisphosphate Against β -Amyloid Induced Neurotoxicity in Rat Hippocampal Organotypic Slice Culture: Involvement of PLC and MEK/ERK Signaling Pathways. Kobe Journal of Medical Science, in press

53) Sakurai T, Yokono K: Comprehensive studies of cognitive impairment of the elderly with diabetes mellitus. Geriatrics and Gerontology International, submitting.

54) Hirano M, Yamasaki K, Okada H, Kitazawa S, Kitazawa R, Ohno Y, Sakurai T, Kondoh T, Ohbayashi C, Katafuchi T, Maeda S, Sugimura K, Tamura S: Estimation of contrast of refraction contrast imaging compared with absorption imaging—basic approach. Radiation Medicine in press.

55) Hirano M, Yamasaki K, Okada H, Sakurai T, Kondoh T, Katafuchi T, Sugimura K, Kitazawa S, Kitazawa R, Maeda S, Tamura S: Ray tracing analysis of overlapping objects in refraction contrast imaging. Radiation Medicine in press.

56) Hirano M, Yamasaki K, Kitazawa R, Kitazawa S, Okada H, Katafuchi K, Maeda S, Sakurai T, Kondoh T, Ohbayashi C, Sugimura K, Tamura S: Imaging of fine structure of bone sample with high coherence X-ray beam and high spatial resolution detector. Radiation Medicine 22: 56-59, 2004

57) Takata T, Yang B, Sakurai T, Okada Y, Yokono K: Glycolysis regulates the induction of lactate utilization for synaptic potentials after hypoxia in the granule cell of guinea pig hippocampus. Neurosci Res. 50:467-74, 2004

中山勝敏

58) Chiba H, Ebihara S, Tomita N, et al. Differential gait kinematics between faller and non-fallers I community-dwelling elderly people. Geriatr Gerontol Internat 5; 127-134, 2005.

59) Kubo H, Nakayama K, Ebihara S, et al. Medical treatments and cares for

geriatric syndrome: new strategies learned from frail elderly. *Tohoku J Exp Med* 205; 205-214, 2005.

60) Iwasaki K, Seki T, Arai H, et al. Combinational western and oriental medicine therapies for geriatric syndrome. *Geriatr Gerontol Int* 5; 216-223, 2005.

61) Yasuda H, Yamaya M, Nakayama K, et al. Carbocysteine reduces frequency of common colds and exacerbations in patients with chronic obstructive pulmonary disease. *J Am Geriatr Soc* 54; 378-380, 2006.

62) Yasuda H, Yamaya M, Nakayama K, et al. Arterial carboxyhemoglobin concentrations as a predictor of chemosensitivity in elderly patients with advanced lung cancer. *J Am Geriatr Soc* 54; 373-375, 2006.

63) Yasuda H, Yamaya M, Nakayama K, Sasaki T, Ebihara S, Kanda A, Asada M, Inoue D, Suzuki T, Takahashi H, Yosida M, Kaneta T, Ishizawa K, Yamada S, Tomita N, Yamasaki M, Kikuchi A, Kubo H, Sasaki H. Randomized phase II trial comparing nitroglycerin plus vinorelbine and cisplatin with vinorelbine and cisplatin alone in previously untreated stage IIIB/IV non-small lung cancer. *J Clin Oncol*. 1;24(4):688-94, 2006

64) Kubo H, Nakayama K, Yanai M, Suzuki T, Yamaya M, Watanabe M, Sasaki H. Anticoagulant therapy for idiopathic pulmonary fibrosis. *Chest*. 128(3) : 1475-82, 2005

63) Yasuda H, Yamaya M, Nakayama K, Ebihara S, Sasaki T, Okinaga S, Inoue D, Asada M, Nemoto M, Sasaki H. Increased Arterial Carboxyhemoglobin Concentrations in Chronic Obstructive Pulmonary Disease. *Am J Respir Crit Care Med*. 1 ; 171(11) : 1246-51, 2005

64) Ohru T, Nakayama K, Fukushima T, Chiba H, Sasaki H. [Prevention of elderly pneumonia by pneumococcal, influenza and BCG vaccinations] *Nippon Ronen Igakkai Zasshi* 42(1):34-6, 2005. Japanese

65) Kikuchi A, Yamaya M, Suzuki S, Yasuda H, Kubo H, Nakayama K, Handa M, Sasaki T, Shibahara S, Sekizawa K, Sasaki H. Association of susceptibility to the development of lung adenocarcinoma with the heme oxygenase-1 gene promoter polymorphism. *Hum Genet* 116(5):354-60, 2005

鈴木裕介

66) Onishi J, Suzuki Y, Umegaki Which Two Questions of Mini-Mental State Examination Should We Start From? *Archives of Gerontology and Geriatrics* (in press) 2006

67) Umegaki H, Yamamoto A, Suzuki Y, Iguchi A Stimulation of the Hippocampal

- Glutamate Receptor Systems Induces Stress-like Responses. *Neuroendocrinology Letters* (in press) 2006
- 68) Umegaki H, Yamaguchi H, Suzuki Y, Iguchi A Microdialysis Measurement of Acetylcholine in Rat Hippocampus during severe Insulin-induced Hypoglycemia. *Neuroendocrinology Letters* (in press) 2006
- 69) Onishi J, Suzuki Y, Umegaki H, Endo H, Kawamura T, Imaizumi M, Iguchi A. Behavioral, Psychological, and Physical Symptoms in Group Homes for the Older Adults with Dementia. *Intl Psychogeriatr* (in press) 2006
- 70) Onishi J, Masuda Y, Suzuki Y, Goto T, Kawamura T, Iguchi A The pleasurable recreational activities among community-dwelling older adults. *Archives of Gerontology and Geriatrics* (in press) 2005
- 71) Iwata M, Kuzuya M, Kitagawa Y, Suzuki Y, Iguchi A Underappreciated predictors for post-discharge mortality in acute hospitalized oldest-old patients. *Gerontology* (in press) 2005
- 72) Onishi J, Suzuki Y, Umegaki H, Endo H, Kawamura T, Iguchi A. A Comparison of Depressive Mood of Older Adults in a Community, Nursing Homes, and a Geriatric Hospital: Factor Analysis of Geriatric Depression Scale. *Journal of Geriatric Psychiatry and Neurology* (in press) 2005
- 73) Onishi J, Masuda Y, Suzuki Y, Endo H, Iguchi A Philadelphia Geriatric Center morale scale in a Japanese nursing home for the elderly. *Geriatr Gerontol Int* (in press) 2005
- 74) Fujishiro H, Umegaki H, Suzuki Y, Oohara-Kurotani S, Yamaguchi Y, Iguchi A. Dopamine D₂ receptor plays a role in memory function: Implications of dopamine-acetylcholine interaction in the ventral hippocampus *Psychopharmacol* 182: 253-61, 2005
- 75) Kuzuya M, Kanda S, Koike T, Suzuki Y, Satake S, Iguchi A. Evaluation of Mini-Nutritional Assessment for Japanese frail elderly. *Nutrition* 21: 498-503, 2005
- 76) Adeli-Rankouhi S, Umegaki H, Zhu W, Suzuki Y, Kurotani-Ohara S, Ieda S, Iguchi A. The entorhinal cortex regulates blood glucose level in response to microinjection of neostigmine into the hippocampus. *Neuroendocrinology Letters* 26: 225-230, 2005
- 77) Kuzuya M, Kanda S, Koike T, Suzuki Y, Satake S, Iguchi A. Lack of correlation between total lymphocyte count and nutritional status in the elderly. *Clin Nutr* 24: 427-432, 2005
- 78) Onishi J, Suzuki Y, Yoshiko K, Hibino S, Iguchi A Predictive Model for the Assessment of Cognitive Impairment by Quantitative Electroencephalography. *Cognitive and Behavioral Neurology* 18: 179-84, 2005
- 79) Onishi J, Suzuki Y, Umegaki H, Nakamura A, Endo H, Iguchi A Influence of behavioral and psychological symptoms of dementia (BPSD) and environment of care on caregivers' burden *Archives of Gerontology and Geriatrics* 41:

159-168, 2005

80) Onishi J, Suzuki Y, Yoshiko K, Hibino S, Iguchi A Predictive Model for the Assessment of Cognitive Impairment by Quantitative Electroencephalography. Cognitive and Behavioral Neurology, (in press), 2004

81) Onishi J, Suzuki Y, Umegaki H, Nakamura A, Endo H, Iguchi A Influence of behavioral and psychological symptoms of dementia (BPSD) and environment of care on caregivers' burden. Archives of Gerontology and Geriatrics (in press) 2004

82) Onishi J, Masuda Y, Suzuki Y, Endo H, Iguchi A Philadelphia Geriatric Center morale scale in a Japanese nursing home for the elderly. Geriatr Gerontol Internatl (in press) 2004

83) Suzuki Y, Yamamoto S, Umegaki H, Onishi J, Mogi N, Fujishiro H, Iguchi A Smell identification test as an indicator for cognitive impairment in Alzheimer's disease

International Journal of Geriatric Psychiatry 19: 727-733, 2004

84) Kanie J, Suzuki Y, Akatsu H, Kuzuya M, Iguchi A. Prevention of late complications by half-solid enteral nutrients in percutaneous endoscopic gastrostomy. Gerontology 50: 417-419, 2004

85) Onishi J, Umegaki H, Suzuki Y, Uemura K, Kuzuya M, Iguchi A The relationship between functional disability and depressive mood in Japanese older adult inpatients.

Journal of Geriatric Psychiatry and Neurology 17(2): 93-98, 2004

86) Yamamoto S, Mogi N, Umegaki H, Suzuki Y, Ando F, Shimokata H, Iguchi A The clock drawing test as a valid screening method for mild cognitive impairment. Dementia and Geriatric Cognitive Disorders 18(2):172-9, 2004

87) Kanie J, Suzuki Y, Akatsu H, Shimokata H, Iguchi A Prevention of gastro-esophageal reflux by an application of half-solid nutrients in patients with percutaneous endoscopic gastrostomy feeding. J Am Geriatr Soc 52(3):466-467, 2004

和文原著、著書

主任研究者

鳥羽研二

1) 鳥羽研二：2. 老化の理解と生き生き長寿。日老医誌 43(1)；65～67, 2006.

Jan

2) 東間紘, 出席者山口脩, 井上裕美, 鳥羽研二：頻尿・尿失禁—中高年の明る

- い過ごし方ー. カレントセラピー 24(1); 90~96, 2006. Jan
- 3) 鳥羽研二: 老化度の測定. 新・老化学 第6章; 111~124, 2005.
- 4) 鳥羽研二: 排尿障害にどうアプローチするか. 治療学 39(11); 1231~1242, 2005. Nov
- 5) 鳥羽研二: 高齢者の排尿障害を巡る問題. 治療学 39(11); 1191~1195, 2005. Nov
- 6) 鳥羽研二: 高齢者高血圧治療とARBの可能性—高齢者高血圧における至適血圧と臓器保護を考える—. Ther. Res. 26(10)1945~1953, 2005. Oct
- 7) 鳥羽研二: 高齢者医療の実情に合った評価法を確立. 性差と医療 2(7); 793~795, 2005. Jul
- 8) 鳥羽研二: 介護予防, 考え方と問題点 介護保険制度の見直しにあたって. 日老医誌 42(4); 383~391, 2005. Jul
- 9) 馬場 幸, 寺本信嗣, 長谷川浩, 町田綾子, 秋下雅弘, 鳥羽研二: 痴呆高齢者に対する嚥下障害のスクリーニング方法の検討: 簡易嚥下誘発試験と反復唾液嚥下テストの比較. 日老医誌 42(3); 323~327, 2005. May
- 10) 鳥羽研二, 大河内二郎, 高橋 泰, 松林公蔵, 西永正典, 山田思鶴, 高橋龍太郎, 西島令子, 小林義雄, 町田綾子, 秋下雅弘, 佐々木英忠: 転倒者ハイリスク者の早期発見の評価方法作成ワーキンググループ: 転倒リスク予測のための「転倒スコア」の開発と妥当性の検証. 日老医誌 42(3); 346~352, 2005. May
- 11) 大内尉義, 寺本信嗣, 鳥羽研二, 秋下雅弘, 長野宏一郎, 江頭正人, 須藤紀子, 井藤英喜, 井上聡, 梅田祐美: 臨床医学の展望 老年医学. 日本醫事新報 4223, 2005. Apr
- 12) 鳥羽研二: 高齢者総合的機能評価とは. Geriat. Med. 43(4); 549~552, 2005. Apr
- 13) 鳥羽研二: 老年症候群, 転倒寝たきり予防のために. 精神経誌 107(4); 354~358, 2005. Apr
- 14) 鳥羽研二: 高齢者総合的機能評価ガイドラインの簡易版を用いて介護予防の推進を. GPnet 51(12); 47~52, 2005. Mar
- 15) 山田思鶴, 鳥羽研二: 痴呆に対するデイ・ケアの効果及び任意選択性作業療法の比較検討. 日老医誌 42(1); 83~89, 2005. Jan
- 16) 鳥羽研二: 高齢者総合的機能評価ガイドライン・理解と臨床的活用法. 医のあゆみ 212(3); 193~196, 2005. Jan
- 17) 鳥羽研二, 西島令子, 小林義雄, 山田思鶴, 大河内二郎, 松林公蔵, 高橋泰, 鈴木裕介, 高橋龍太郎, 佐々木英忠: 転倒ハイリスク者の早期発見のための「転倒スコア」の開発と有用性の検討. Osteoporos Jpn 13(1); 68~71, 2005. Jan

- 18) 鳥羽研二：アルツハイマー病と生活習慣、とくに運動習慣. *Dementia Jpn* 18(3) ; 205~210, 2004.
- 19) 鳥羽研二：痴呆患者の総合的機能評価・老年医学的立場から. *Progress in Medicine* 24(10) ; 25~29, 2004. Oct
- 20) 鳥羽研二：高齢者失禁の診断のポイント. *J Clin Rehabil* 13(9) ; 795~799, 2004. Sep
- 21) 青木千夏, 水川真二郎, 土屋一洋, 田澤涼, 園原和樹, 竹下実希, 秋下雅弘, 大荷満生, 鳥羽研二：髄膜炎の経過中に脳室炎を合併したMDSの1例. *Geriatr Med* 42(8) ; 1057~1059, 2004. Aug
- 22) 鳥羽研二：老年症候群とは何か. *治療学* 38(7) ; 14~17, 2004. Jul
- 23) 鳥羽研二：「もの忘れ外来」の実態・老年病科の立場から. *Geriatr Med* 42(6) ; 57~62, 2004. Jun
- 24) 秋下雅弘, 寺本信嗣, 荒井秀典, 荒井啓行, 水上勝義, 森本茂人, 鳥羽研二：大学病院老年科における薬物有害作用の実態調査. *日老医誌* 41(3) ; 303~306, 2004. May

分担研究者

松田晋哉

- 25) 松田晋哉：介護予防入門（2005）、社会保険研究所., No. 2238 : 12-18.
- 26) 松田晋哉：介護予防の考え方, 北海道公衆衛生雑誌（2005）, 18(2) : 12-17.
- 27) 松田晋哉：健康づくり推進のための総合データベース構築の必要性, 社会保険旬報（2005）, No. 2256 : 18-24.
- 28) 松田晋哉：介護予防を考える（上）, 介護保険情報（2004）, 2004. 8月号 : 66-70.
- 29) 松田晋哉：介護予防を考える（上）, 介護保険情報（2004）, 2004. 7月号 : 66-70.
- 30) 松田晋哉：亜急性期医療の考え方, 月刊/保険診療, 59(6) : 81-85.
- 31) 松田晋哉：まちづくりの視点からみた介護予防における課題, 介護保険情報（2004）, 2004. 5月号 : 66-72.

山田思鶴

- 32) 山田思鶴, 鳥羽研二：痴呆に対するデイ・ケアの効果及び任意選択性作業療法の比較検討. *日老医誌* 42(1) ; 83~89, 2005. Jan

櫻井 孝

- 33) 向田善之、櫻井 孝、横野浩一：高齢者糖尿病予防・治療・ケアー認知機能

障害. 日本臨床 64 : 119-123, 2006

34) 芳野 弘、櫻井 孝、横野浩一：合併症のある痴呆患者への対応（その1）糖尿病. Dementia & Nicotinic acetylcholine receptor Trends 8: 6-7, 2006

35) 櫻井 孝、横野浩一：老年医学教育からみた老年病専門医の役割. 日本老年医学会雑誌 印刷中

36) 櫻井 孝：透析患者の神経系の異常. 透析ガイドライン 深川雅史編 印刷中

37) 明寄太一、櫻井 孝：危険因子の適正評価—認知機能障害. 介護予防ガイドライン 鳥羽研二編 印刷中

38) 上野正夫、櫻井 孝：要介護者、虚弱者の定義と分類—認知機能面 (AACD・MCI 認知症)での区分. 介護予防ガイドライン 鳥羽研二編 印刷中

39) 向田善之、櫻井 孝、横野浩一：危険因子の適正評価—メタボリックシンドローム. 介護予防ガイドライン 鳥羽研二編 印刷中

40) 芳野 弘、櫻井 孝：認知症予防. 介護予防ガイドライン 鳥羽研二編 印刷中

41) 明寄太一、櫻井 孝、横野浩一：高齢者糖尿病における認知機能障害の成因. 内分泌・糖尿病科 20 : 81-7, 2005

42) 櫻井 孝、倉永雅子：総合的機能評価を生かした初診外来 物忘れ外来. 老年医学 42 : 178-182, 2004

43) 櫻井 孝、宋 秀珍：老年医学と介護保険. 日本老年医学会雑誌 41 : 189-192, 2004

44) 明寄太一、櫻井 孝、横野浩一：高齢者における生活習慣病と多臓器不全. 老年医学 42 : 419-424, 2004

45) 櫻井 孝：生活習慣病と老年期痴呆. 治療学 38 : 24, 2004

46) 横野浩一、櫻井 孝：高齢者糖尿病の治療と研究. 日老医誌 41 : 369-371, 2004

47) 櫻井 孝、横野浩一：高齢者における知的機能・運動機能の変化. プラクティス 21 : 520-528, 2004

鈴木裕介

48) 蟹江治郎、赤津裕康、鈴木裕介：胃瘻チューブ交換時に生じた腹腔内誤挿入に対し外来処置のみで対処が可能であった1例. 日本老年医学会雑誌 42 : 698-701, 2005

49) 蟹江治郎、鈴木裕介、赤津裕康、各務千鶴子 固形化経腸栄養剤の実施における栄養剤の安定性と安全性の評価—調理によるビタミンの変化と細菌学的変化— 静脈経腸栄養 19 (1) : 65-69, 2004



Angiotensin converting enzyme inhibitor attenuates oxidative stress-induced endothelial cell apoptosis via p38 MAP kinase inhibition

Wei Yu^a, Masahiro Akishita^{b,*}, Hang Xi^a, Kumiko Nagai^a, Noriko Sudoh^a,
Hiroshi Hasegawa^a, Koichi Kozaki^a, Kenji Toba^a

^a Department of Geriatric Medicine, Kyorin University School of Medicine, Tokyo, Japan

^b Department of Geriatric Medicine, Graduate School of Medicine, University of Tokyo, 7-3-1 Hongo, Bunkyo-ku, Tokyo 113-8655, Japan

Received 11 May 2005; received in revised form 22 July 2005; accepted 29 July 2005

Available online 8 September 2005

Abstract

Background: The effects of angiotensin converting enzyme (ACE) inhibitors on oxidative stress-induced apoptosis of endothelial cells and the intracellular signaling were investigated.

Methods: Cultured endothelial cells derived from a bovine carotid artery were treated with H₂O₂ or TNF- α to induce apoptosis. Apoptosis was evaluated by DNA fragmentation and cell viability, p38 MAP kinase activity by Western blotting, and oxidative stress by formation of 8-isoprostane. The effects of ACE inhibitors were examined by adding them into the medium throughout the experiments.

Results: Apoptosis was attenuated by ACE inhibitors, temocapril and captopril, in a dose-dependent manner (1–100 μ mol/l). H₂O₂ (0.2 mmol/l for 1.5 h) or TNF- α (10 ng/ml for 72 h) treatment stimulated the activities of p38 MAP kinase. Temocapril and captopril decreased the activity of p38 MAP kinase as well as 8-isoprostane formation induced by H₂O₂. A p38 MAP kinase inhibitor, SB203580, partially inhibited the effect of temocapril on apoptosis.

Conclusions: These results suggest that ACE inhibitors protect endothelial cells from oxidative stress-induced apoptosis, and that p38 MAP kinase plays a critical role in the process.

© 2005 Elsevier B.V. All rights reserved.

Keywords: Apoptosis; ACE inhibitor; Endothelial cell; p38 MAP kinase

1. Introduction

Stress-induced injury of vascular endothelial cells (ECs) is considered to be an initial event in the development of atherosclerosis [1]. In particular, oxidative stress has been implicated in endothelial injury caused by oxidized LDL and smoking as well as hypertension, diabetes and ischemia-reperfusion [1–3]. This notion is supported by the findings that the production of reactive oxygen species is upregulated in vascular lesions [4,5], and that lesion formation such as endothelial dysfunction is accelerated by superoxide anion [6] and, in contrast, is attenuated by free radical scavengers including vitamin E [7] and superoxide dismutase [8].

Angiotensin converting enzyme (ACE) inhibitors effectively interfere with the renin angiotensin system and exert various beneficial actions on vascular structure and function beyond their blood pressure-lowering effects [9,10]. ACE inhibitors attenuate neointimal formation after vascular injury in animals [11] and endothelial dysfunction in humans [12]. It has been demonstrated that ACE activation induces oxidative stress [13]. However, it has not been elucidated whether ACE inhibitors could attenuate oxidative stress-induced EC apoptosis, an initial and important process in atherosclerosis [14,15].

In this study, we examined the effects of ACE inhibitors, temocapril and captopril, on H₂O₂- and TNF- α -induced EC apoptosis and the pro-apoptotic intracellular signaling, p38 mitogen-activated protein (MAP) kinase, to clarify the underlying mechanism.

* Corresponding author. Tel.: +81 3 5800 8832; fax: +81 3 5800 8831.
E-mail address: akishita-iky@umin.ac.jp (M. Akishita).

2. Materials and methods

2.1. Induction of EC apoptosis

ECs derived from a bovine carotid artery [16] was cultured in Dulbecco's modified Eagle medium (Gibco) supplemented with 10% fetal bovine serum. Cells were maintained at 37 °C in a 95% air/5% CO₂ atmosphere. ECs of the 5th to 7th passage were used in the experiments. When the cells had grown to 70–80% confluence, ECs were pretreated for 24 h with culture medium containing the reagents that were tested in the experiments. Subsequently, after washing twice with Hank's balanced salt solution (Gibco), the cells were exposed to H₂O₂ (0.1–0.4 mmol/l) diluted in Hank's balanced salt solution for 1.5 h at 37 °C to induce apoptosis. The cells were washed three times with Hank's balanced salt solution, and then cultured in culture medium containing the reagents until assay. Similarly, tumor necrosis factor- α (TNF- α , 5–20 ng/ml; Sigma) was added to the medium until assay

after 24-h pretreatment with the reagents tested. EC viability and apoptosis were evaluated at 24 h after H₂O₂ treatment, or at 72 h after TNF- α treatment. The effects of temocapril (1–100 μ mol/l) and captopril (1–100 μ mol/l) were examined by adding them into the medium throughout the experiments. The effect of a specific p38 MAP kinase inhibitor, SB203580 (10 μ mol/l; Calbiochem), was examined by treating ECs with SB203580 for 1 h before H₂O₂ treatment.

2.2. Cell viability

Cell viability was estimated using an MTT (3-(4,5-dimethylthiazol-2-yl)-2,5-diphenyltetrazolium bromide; Sigma) assay [17]. Briefly, 1 mg/ml MTT (final concentration) was added to the well and incubated for 2 h at 37 °C. The medium was removed and cells were lysed with 2-isopropanol containing 0.04 mol/l HCl. The absorbance measured at 595 nm was used to calculate the relative cell viability ratio.

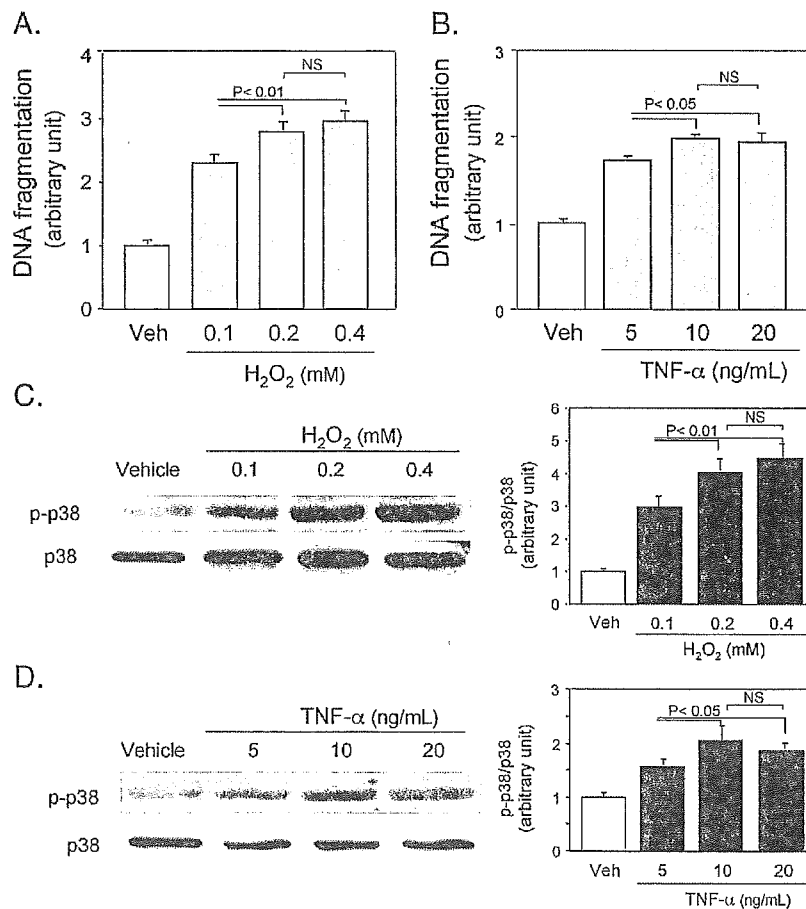


Fig. 1. Dose-dependent effects of H₂O₂ (A, C) and TNF- α (B, D) on EC apoptosis (A, B) and p38 MAP kinase activity (C, D). A and B, apoptosis was evaluated 24 h after H₂O₂ treatment (for 1.5 h) or 72 h after addition of TNF- α by means of DNA fragmentation ($n=3$). C and D, the activity of p38 MAP kinase was evaluated by immunoblotting using the specific antibody against the phosphorylated form of the kinase (p-p38) at 30 min after addition of H₂O₂ or TNF- α . Right panels show the results of densitometric analyses of immunoblotting (mean \pm SEM, $n=3$). NS, not significant. Values are expressed as mean \pm SEM ($n=3$).

2.3. Evaluation of EC apoptosis and formation of 8-isoprostane

For quantitative determination, EC apoptosis was measured as DNA fragmentation. DNA fragmentation was evaluated by histone-associated DNA fragments using a photometric enzyme immunoassay (Cell Death Detection ELISA, Roche), according to the manufacturer's instructions. Briefly, attached cells were harvested with trypsin, and the cell suspension was pelleted by centrifugation. Floating and attached cells were lysed. After centrifugation, the supernatant was measured by ELISA.

Formation of 8-isoprostane (8-*iso* prostaglandin $F_{2\alpha}$) was measured using a commercially available EIA kit (Cayman Chemical). Culture supernatants were diluted with EIA buffer when necessary, and were applied to EIA according to the manufacturer's instructions.

2.4. Immunoblotting

The cells were washed twice with ice-cold phosphate-buffered saline and lysed in lysis buffer (25 mmol/l Tris/HCl, pH 7.5, 25 mmol/l NaCl, 0.5 mmol/l EGTA, 10 mmol/l NaF, 20 mmol/l β -glycerophosphate, 1 mmol/l Na_3VO_4 , 1 mmol/l

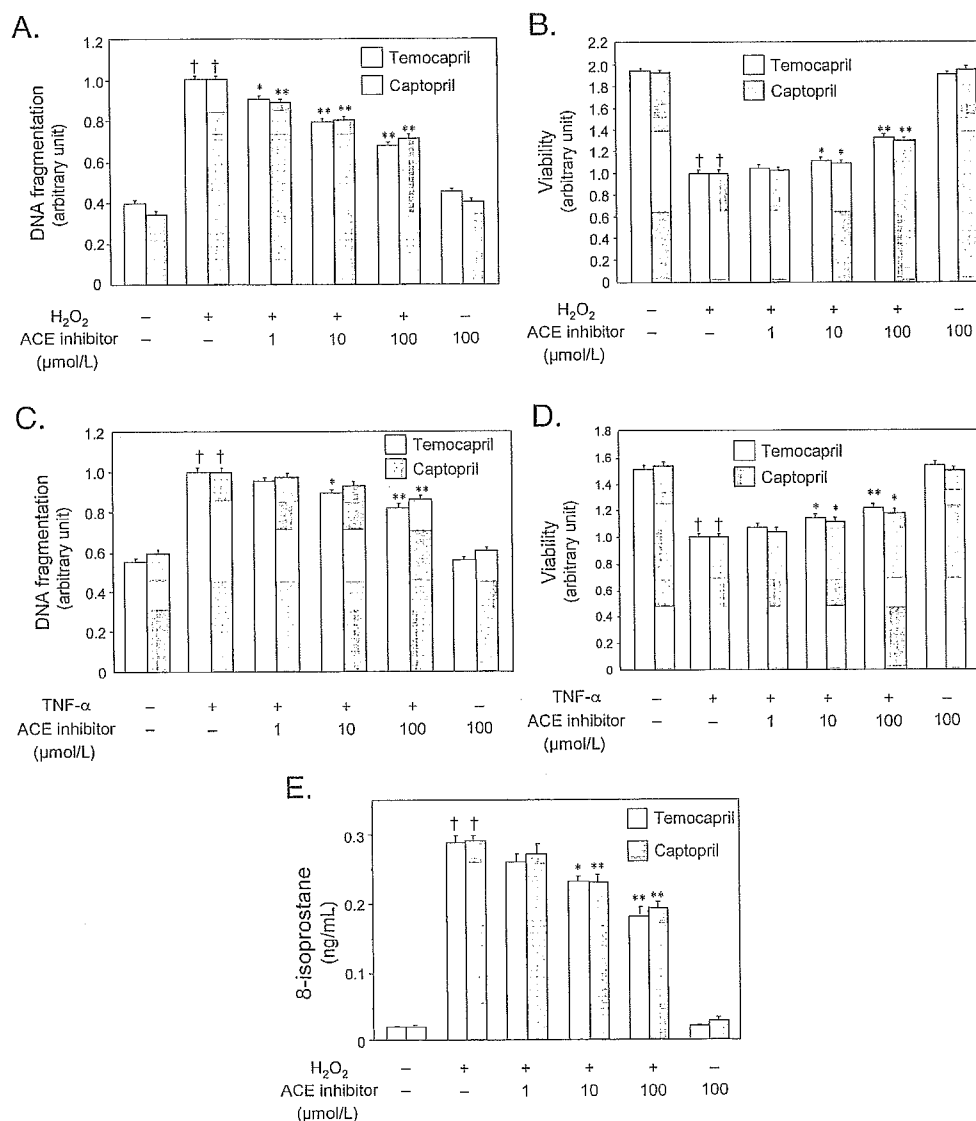


Fig. 2. Effects of ACE inhibitors on H₂O₂-induced (A, B) and TNF- α -induced (C, D) EC apoptosis and the effects of ACE inhibitors on H₂O₂-induced 8-isoprostane formation (E). Temocapril, captopril or their vehicle was added to the culture medium 24 h before H₂O₂ or TNF- α treatment until assay. Apoptosis (A, C) and cell viability (B, D) were evaluated 24 h after H₂O₂ treatment (0.2 mmol/l for 1.5 h) or 72 h after TNF- α treatment (10 ng/ml for 72 h) by means of DNA fragmentation ($n=3$) and MTT assay ($n=8$), respectively. 8-Isoprostane concentration (E; $n=3$) in the culture supernatant was measured 3 h after H₂O₂ treatment. A and B, † $P<0.01$ vs. H₂O₂ (-). * $P<0.05$, ** $P<0.01$ vs. H₂O₂ (+)+ACE inhibitor (-). C and D, † $P<0.01$ vs. TNF- α (-). * $P<0.05$, ** $P<0.01$ vs. TNF- α (+)+ACE inhibitor (-). Values are expressed as mean \pm SEM. Similar results were obtained in three independent experiments.

PMSF, and 10 $\mu\text{g/ml}$ aprotinin) at 4 °C. After sonication and centrifugation at 15,000 rpm, the supernatant was used for the following immunoblotting. The lysate (20 μg protein per lane) was separated on 12% SDS-polyacrylamide gel, electroblotted onto nitrocellulose membrane, and immunoblotted with specific primary antibodies, both of which were purchased from Cell Signaling Technology (Beverly, MA). The antibodies used in this study were anti-phospho-p38 MAP kinase (phospho-p38 28B10 #9216) and anti-p38 MAP kinase (#9212). Antibodies were detected by means of a horseradish peroxidase-linked secondary antibody using an enhanced chemiluminescence system (Amersham Pharmacia Biotech). Densitometric analysis was performed using an image scanner and analyzing software (NIH image ver. 1.61). The activity of each kinase was evaluated by calculating the ratio of the amount of the phosphorylated form to that of the total form.

2.5. Data analysis

The values are expressed as mean \pm SEM in the text and figures. Data were analyzed using one-factor ANOVA. If a

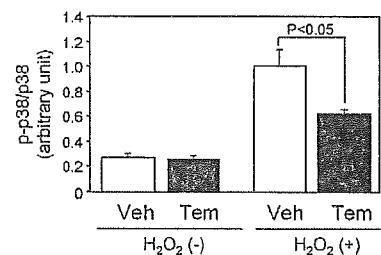
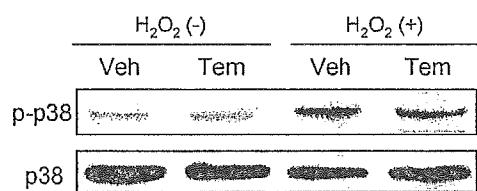
statistically significant effect was found, Newman–Keuls' test was performed to isolate the difference between the groups. Differences with a value of $P < 0.05$ were considered statistically significant.

3. Results

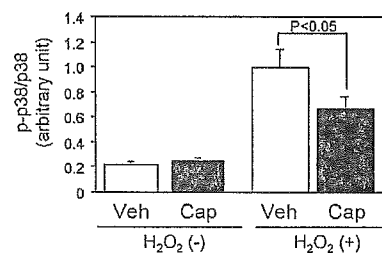
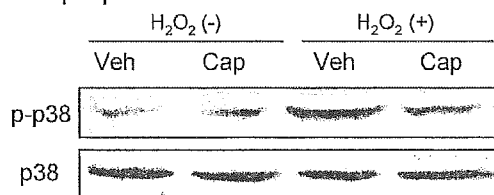
3.1. Dose-dependent effects of H_2O_2 and $\text{TNF-}\alpha$ on EC apoptosis and p38 MAP kinase activity

Increasing concentrations of H_2O_2 and $\text{TNF-}\alpha$ were applied to examine the effects on EC apoptosis and p38 MAP kinase activity. Based on the literature [18] and time–response experiments (data not shown), EC apoptosis was evaluated at 24 h after H_2O_2 treatment for 1.5 h, or at 72 h after addition of $\text{TNF-}\alpha$. The activity of p38 MAP kinase, as measured by immunoblotting using the specific antibody against the phosphorylated form of the kinase, was evaluated at 30 min after addition of H_2O_2 or $\text{TNF-}\alpha$, based on time–response experiments (data not shown). As shown in Fig. 1A–D, the effects of H_2O_2 and $\text{TNF-}\alpha$ were

A. Temocapril



B. Captopril



C. Olmesartan

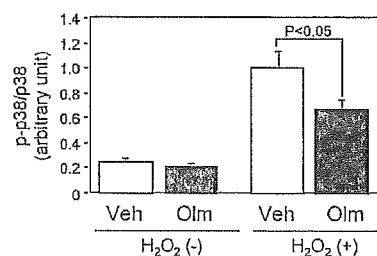
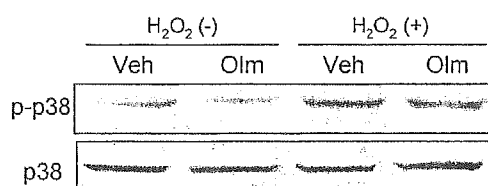


Fig. 3. Effects of temocapril (A), captopril (B) and olmesartan (C) on p38 MAP kinase activity at 30 min after exposure to H_2O_2 . Temocapril (100 $\mu\text{mol/l}$), captopril (100 $\mu\text{mol/l}$), olmesartan (10 $\mu\text{mol/l}$) or its vehicle was added to the culture medium 24 h before H_2O_2 treatment until assay. Right panels show the results of densitometric analyses of immunoblotting (mean \pm SEM, $n = 3$).

dose dependent, but there was no significant further increase in EC apoptosis and p38 MAP kinase activity by H_2O_2 of >0.2 mmol/l or by TNF- α of >10 ng/ml. Based on these data, the following experiments were examined using 0.2 mmol/l H_2O_2 or 10 ng/ml TNF- α .

3.2. Effect of ACE inhibitors on EC apoptosis

EC apoptosis, as measured by DNA fragmentation, was significantly attenuated by temocapril and captopril in a dose-dependent manner (Fig. 2A). Reflecting this effect, cell viability was ameliorated by addition of temocapril and captopril in a dose-dependent manner (Fig. 2B).

We also tested using TNF- α whether anti-apoptotic effects of ACE inhibitors would be specific to H_2O_2 or not. As shown in Fig. 2C, both temocapril and captopril effectively inhibited EC apoptosis in a dose-dependent manner. This was associated with the recovery of cell viability by the ACE inhibitors (Fig. 2D). Throughout the experiments, the effects of temocapril were comparable to those of captopril.

To confirm the antioxidant effects of temocapril and captopril, the formation of 8-isoprostane, a marker of oxidative stress, was measured. Temocapril and captopril restrained 8-isoprostane formation induced by H_2O_2 in a dose-dependent manner (Fig. 2E).

3.3. Effect of ACE inhibitor on p38 MAP kinase activity

Next, the effects of ACE inhibitors on p38 MAP kinase activity were examined because the kinase has been implicated in the cell signaling leading to apoptosis [14,19,20]. As shown in Fig. 3A,B, temocapril and captopril decreased the activity of p38 MAP kinase at 30 min after H_2O_2 treatment by approximately 30–40% without any change in the total protein. An AT1 receptor blocker,

olmesartan, showed similar effects on p38 MAP kinase activity (Fig. 3C).

Finally, the effect of a p38 MAP kinase inhibitor, SB203580, was examined. SB203580 reduced H_2O_2 -induced EC apoptosis by 20%. More importantly, SB203580 partially but significantly inhibited the effect of temocapril on apoptosis (Fig. 4). Taking these results together with the pro-apoptotic action of p38 MAP kinase, it is suggested that p38 MAP kinase is involved in the effect of temocapril on EC apoptosis.

4. Discussion

A number of investigations have shown that angiotensin II induces oxidative stress in ECs. Angiotensin II stimulates the production of reactive oxygen species in ECs by upregulating the subunits of NAD(P)H oxidase, gp91 phox [21] and p47 phox [22]. It has been reported that the renin angiotensin system contributes to endothelial dysfunction in patients with renovascular hypertension [23]. Conversely, it has been shown experimentally that ACE inhibitors can reduce the production of reactive oxygen species in pathological conditions such as peripheral arteries in rats with chronic heart failure [24], rat diabetic nephropathy [25] and kidney mitochondria in aged rats [26]. In the clinical setting, 4-week treatment with ramipril, in patients with coronary artery disease, diminished the response of endothelium-dependent vasodilation to intracoronary administration of antioxidant vitamin C in parallel with improvement of basal endothelium-dependent vasodilation [27], indicating that ACE inhibitors can improve endothelial function in association with a reduction of oxidative stress.

In the present study, we investigated EC apoptosis, an important process that leads to endothelial dysfunction and atherosclerosis [14,15], and showed that ACE inhibitors, temocapril and captopril, attenuated EC apoptosis induced by H_2O_2 as well as by TNF- α . This result indicates that anti-apoptotic effects of ACE inhibitors are not specific to H_2O_2 , but might be attributable to the anti-oxidant action of ACE inhibitors, because reactive oxygen species are known to be involved in TNF- α -induced EC apoptosis [28,29]. Reduction in 8-isoprostane formation by temocapril and captopril further supports the anti-oxidant effects of ACE inhibitors. It is not likely that the anti-apoptotic effects of ACE inhibitors were mediated through nitric oxide production via the inhibition of bradykinin degradation [11], because a nitric oxide synthase inhibitor, *N*^G-nitro-L-arginine methyl ester, did not influence the effect of temocapril on EC apoptosis (data not shown). Rather, the effects of ACE inhibitors are likely to be mediated through inhibition of angiotensin II production, as was demonstrated by the effect of olmesartan on p38 MAP kinase.

Reactive oxygen species activate many kinds of intracellular signaling, resulting in the transcription of numerous genes and the modulation of cellular function [30]. As

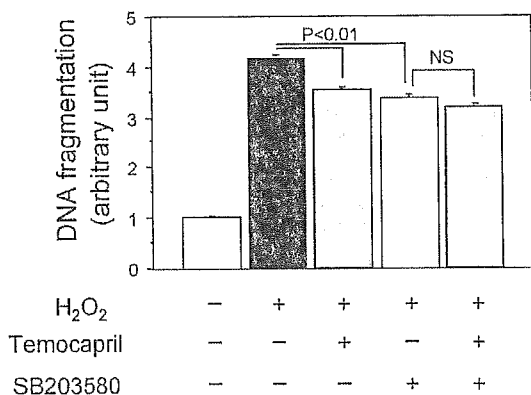


Fig. 4. Effects of temocapril and SB203580 on H_2O_2 -induced EC apoptosis. Temocapril (100 μ mol/l) or its vehicle was added to the culture medium 24 h before H_2O_2 treatment until assay. SB203580 (10 μ mol/l) or its vehicle was added to the culture medium for 1 h before H_2O_2 treatment. EC apoptosis was determined by DNA fragmentation 24 h after H_2O_2 treatment. NS, not significant. Values are expressed as mean \pm SEM ($n=3$). Similar results were obtained in three independent experiments.

previously reported [31–33], extracellular signal-regulated kinase (ERK), c-Jun N-terminal kinase (JNK) and Akt in addition to p38 MAP kinase were activated in ECs by exposure to H₂O₂ (data not shown). Of these serine/threonine kinases, we focused on p38 MAP kinase because p38 MAP kinase is pro-apoptotic signaling, while ERK and Akt are anti-apoptotic, and JNK is anti- or pro-apoptotic depending on conditions [14,19,20]. We found that both temocapril and captopril inhibited the activity of p38 MAP kinase induced by H₂O₂. Although p38 MAP kinase is activated by stress and cytokines and acts on various target proteins, little is known about the downstream signaling [19,20,34]. However, EC apoptosis was effectively blocked in studies using a p38 MAP kinase inhibitor [35,36] and a dominant-negative form of p38 MAP kinase [35], indicating that activation of p38 MAP kinase leads to EC apoptosis. As a matter of fact, a p38 MAP kinase inhibitor, SB203580, partially inhibited H₂O₂-induced EC apoptosis in the present study. More importantly, SB203580 partially but significantly inhibited the effect of temocapril on apoptosis, further implying the role of p38 MAP kinase in the effect of temocapril. However, the partial effects of SB203580 also suggest the role of other pathways than p38 MAP kinase. We should perform future studies to determine the exact mechanism underlying H₂O₂-induced EC apoptosis.

In summary, we found that ACE inhibitors attenuated oxidative stress-induced EC apoptosis in culture. Furthermore, it was suggested that p38 MAP kinase was critical in the inhibitory effect of temocapril on EC apoptosis. These findings provide a mechanistic insight into the effects of ACE inhibitors, which have been used for the treatment of cardiovascular disease.

Acknowledgements

We thank Ms. Mariko Sawano for her excellent technical assistance. This study was supported by a Grant-in-Aid for Scientific Research from the Ministry of Education, Science, Culture and Sports of Japan (13670741), and by Health and Labour Sciences Research Grants (H16-Choju-013 and H16-Choju-015) from the Ministry of Health, Labour and Welfare of Japan.

References

- [1] Ross R. Atherosclerosis—an inflammatory disease. *N Engl J Med* 1999;340:115–26.
- [2] Griendling KK, Sorescu D, Lassegue B, Ushio-Fukai M. Modulation of protein kinase activity and gene expression by reactive oxygen species and their role in vascular physiology and pathophysiology. *Arterioscler Thromb Vasc Biol* 2000;20:2175–83.
- [3] Zalba G, San Jose G, Moreno MU, et al. Oxidative stress in arterial hypertension: role of NAD(P)H oxidase. *Hypertension* 2001;38:1395–9.
- [4] Sorescu D, Weiss D, Lassegue B, et al. Superoxide production and expression of nox family proteins in human atherosclerosis. *Circulation* 2002;105:1429–35.
- [5] Spiekermann S, Landmesser U, Dikalov S, et al. Electron spin resonance characterization of vascular xanthine and NAD(P)H oxidase activity in patients with coronary artery disease: relation to endothelium-dependent vasodilation. *Circulation* 2003;107:1383–9.
- [6] Rey FE, Li XC, Carretero OA, Garvin JL, Pagano PJ. Perivascular superoxide anion contributes to impairment of endothelium-dependent relaxation: role of gp91(phox). *Circulation* 2002;106:2497–502.
- [7] Pratico D, Tangirala RK, Rader DJ, Rokach J, FitzGerald GA. Vitamin E suppresses isoprostane generation in vivo and reduces atherosclerosis in ApoE-deficient mice. *Nat Med* 1998;4:1189–92.
- [8] Fennell JP, Brosnan MJ, Frater AJ, et al. Adenovirus-mediated overexpression of extracellular superoxide dismutase improves endothelial dysfunction in a rat model of hypertension. *Gene Ther* 2002;9:110–7.
- [9] Unger T. Blood pressure lowering and renin–angiotensin system blockade. *J Hypertens* 2003;6:S3–7.
- [10] Scribner AW, Loscalzo J, Napoli C. The effect of angiotensin-converting enzyme inhibition on endothelial function and oxidant stress. *Eur J Pharmacol* 2003;482:95–9.
- [11] Akishita M, Shirakami G, Iwai M, et al. Angiotensin converting enzyme inhibitor restrains inflammation-induced vascular injury in mice. *J Hypertens* 2001;19:1083–8.
- [12] Antony I, Lerebours G, Nitenberg A. Angiotensin-converting enzyme inhibition restores flow-dependent and cold pressor test-induced dilations in coronary arteries of hypertensive patients. *Circulation* 1996;94:3115–22.
- [13] Warmholtz A, Nickenig G, Schulz E, et al. Increased NADH-oxidase-mediated superoxide production in the early stages of atherosclerosis: evidence for involvement of the renin–angiotensin system. *Circulation* 1999;99:2027–33.
- [14] Choy JC, Granville DJ, Hunt DW, McManus BM. Endothelial cell apoptosis: biochemical characteristics and potential implications for atherosclerosis. *J Mol Cell Cardiol* 2001;33:1673–90.
- [15] Dimmeler S, Haendeler J, Zeiher AM. Regulation of endothelial cell apoptosis in atherothrombosis. *Curr Opin Lipidol* 2002;13:531–6.
- [16] Akishita M, Kozaki K, Eto M, et al. Estrogen attenuates endothelin-1 production by bovine endothelial cells via estrogen receptor. *Biochem Biophys Res Commun* 1998;251:17–21.
- [17] Dimmeler S, Haendeler J, Nehls M, Zeiher AM. Suppression of apoptosis by nitric oxide via inhibition of interleukin-1beta-converting enzyme (ICE)-like and cysteine protease protein (CPP)-32-like proteases. *J Exp Med* 1997;185:601–7.
- [18] Grethe S, Ares MP, Andersson T, Porn-Ares MI. p38 MAPK mediates TNF-induced apoptosis in endothelial cells via phosphorylation and downregulation of Bcl-x(L). *Exp Cell Res* 2004;298:632–42.
- [19] Johnson GL, Lapadat R. Mitogen-activated protein kinase pathways mediated by ERK, JNK, and p38 protein kinases. *Science* 2002;298:1911–2.
- [20] Cross TG, Scheel-Toellner D, Henriquez NV, Deacon E, Salmon M, Lord JM. Serine/threonine protein kinases and apoptosis. *Exp Cell Res* 2000;256:34–41.
- [21] Rueckschloss U, Quinn MT, Holtz J, Morawietz H. Dose-dependent regulation of NAD(P)H oxidase expression by angiotensin II in human endothelial cells: protective effect of angiotensin II type 1 receptor blockade in patients with coronary artery disease. *Arterioscler Thromb Vasc Biol* 2002;22:1845–51.
- [22] Landmesser U, Cai H, Dikalov S, et al. Role of p47(phox) in vascular oxidative stress and hypertension caused by angiotensin II. *Hypertension* 2002;40:511–5.
- [23] Higashi Y, Sasaki S, Nakagawa K, Matsuura H, Oshima T, Chayama K. Endothelial function and oxidative stress in renovascular hypertension. *N Engl J Med* 2002;346:1954–62.
- [24] Varin R, Mulder P, Tamion F, et al. Improvement of endothelial function by chronic angiotensin-converting enzyme inhibition in heart

- failure: role of nitric oxide, prostanoids, oxidant stress, and bradykinin. *Circulation* 2000;102:351–6.
- [25] Onozato ML, Tojo A, Goto A, Fujita T, Wilcox CS. Oxidative stress and nitric oxide synthase in rat diabetic nephropathy: effects of ACEI and ARB. *Kidney Int* 2002;61:186–94.
- [26] de Cavanagh EM, Piotrkowski B, Basso N, et al. Enalapril and losartan attenuate mitochondrial dysfunction in aged rats. *FASEB J* 2003;17:1096–8.
- [27] Hornig B, Landmesser U, Kohler C, et al. Comparative effect of ace inhibition and angiotensin II type 1 receptor antagonism on bioavailability of nitric oxide in patients with coronary artery disease: role of superoxide dismutase. *Circulation* 2001;103:799–805.
- [28] Kofler S, Nickel T, Weis M. Role of cytokines in cardiovascular diseases: a focus on endothelial responses to inflammation. *Clin Sci (Lond)* 2005;108:205–13.
- [29] Shakibaei M, Schulze-Tanzil G, Takada Y, Aggarwal BB. Redox regulation of apoptosis by members of the TNF superfamily. *Antioxid Redox Signal* 2005;7:482–96.
- [30] Griendling KK, Sorescu D, Lassegue B, Ushio-Fukai M. Modulation of protein kinase activity and gene expression by reactive oxygen species and their role in vascular physiology and pathophysiology. *Arterioscler Thromb Vasc Biol* 2000;20:2175–83.
- [31] Huot J, Houle F, Rousseau S, Deschesnes RG, Shah GM, Landry J. SAPK2/p38-dependent F-actin reorganization regulates early membrane blebbing during stress-induced apoptosis. *J Cell Biol* 1998;143:1361–73.
- [32] Chen K, Vita JA, Berk BC, Keaney Jr JF. c-Jun N-terminal kinase activation by hydrogen peroxide in endothelial cells involves SRC-dependent epidermal growth factor receptor transactivation. *J Biol Chem* 2001;276:16045–50.
- [33] Thomas SR, Chen K, Keaney Jr JF. Hydrogen peroxide activates endothelial nitric-oxide synthase through coordinated phosphorylation and dephosphorylation via a phosphoinositide 3-kinase-dependent signaling pathway. *J Biol Chem* 2002;277:6017–24.
- [34] Shi Y, Gaestel M. In the cellular garden of forking paths: how p38 MAPKs signal for downstream assistance. *Biol Chem* 2002;383:1519–36.
- [35] Nakagami H, Morishita R, Yamamoto K, et al. Phosphorylation of p38 mitogen-activated protein kinase downstream of bax-caspase-3 pathway leads to cell death induced by high D-glucose in human endothelial cells. *Diabetes* 2001;50:1472–81.
- [36] Takahashi M, Okazaki H, Ogata Y, Takeuchi K, Ikeda U, Shimada K. Lysophosphatidylcholine induces apoptosis in human endothelial cells through a p38-mitogen-activated protein kinase-dependent mechanism. *Atherosclerosis* 2002;161:387–94.

Editor-Communicated Paper

Analysis of the Distribution of Neuropathogenic Retroviral Antigens Following PVC211 or A8-V Infection

Ryuhei Nakai¹, Sayaka Takase-Yoden², and Rihito Watanabe^{*,2}

¹Department of Geriatric Medicine, Kyorin University School of Medicine, Mitaka, Tokyo 181–8611, Japan, and ²Department of Bioinformatics, Faculty of Engineering, Soka University, Hachioji, Tokyo 192–8577, Japan

Communicated by Dr. Hiroshi Kida; Received September 14, 2005. Accepted October 6, 2005

Abstract: A8-V and PVC211 are neuropathogenic strains of the Friend murine leukemia virus (Fr-MLV) that cause spongiosis in the rat brain after infection at birth. PVC211 exhibited stronger neuropathogenicity than A8-V, and induced more severe neurological symptoms such as hind-leg paralysis. These symptoms correlated with the neuropathological spread and intensity, which were more severe in the spinal cord of rats infected with PVC211 than in those infected with A8-V, without exhibiting neuropathological differences in other areas of the CNS. Interestingly, virus titers recovered from infected spinal cords were similar in PVC211 and A8-V infected animals. However, in the spinal cord infected with PVC211, glial cells attained higher immunohistochemical expression scores for the viral surface antigen, gp70 (Env) than in the A8-V infected spinal cord, although expression levels of viral antigens in blood vessel walls were similar in A8-V and PVC211 infections. Furthermore, many of those glial cells which carried viral antigens were found, by double immunostaining, to be microglia. The results suggested that the spread of viral antigen positive microglia plays an important role in forming the different neuro-pathogenicity observed in A8-V and PVC211 infections.

Key words: Ecotropic, Histochemistry, CNS

The FrC6-V, from which A8-V was molecularly cloned (15), and the PVC211 (5) were separately isolated by different methods (20) from the same source of the Fr-MLV complex which had been maintained by mouse-to-mouse passages for over 30 times (10). The A8-V shares a high degree of homology with PVC211 in the R (98.5%), U5 (100%), 5' leader (99.6%), *gag* (99.6%), *pol* (99.5%), and *env* (99.7%) regions (15). The lowest degree of homology between the A8 virus and PVC211 is in the U3 region of the LTR (81.4%). This low homology was attributed to differences in enhancer elements in the U3 region (15). But our recent study using recombinant viruses revealed that the enhancer elements of the neuropathogenic viruses do not contribute to their neuropathogenicity (19), although A8-V enhancer elements appeared to be responsible for its ability to proliferate at high rates in

the CNS and to induce tumorigenesis in the thymus and spleen (18).

One common feature of A8-V and PVC211 is that the primary determinant for the induction of neurodegenerative disease is the *env* gene, but other viral genes also have effects on neuropathogenicity (15). The 0.3-kb fragment containing 0.04-kb of R, U5, and the 5' half of the 5' leader of A8 are essential for the induction of spongiform neurodegeneration (19). In the case of PVC211, the sequences within the 5' leader sequence, the *gag* gene, and the 5' quarter of the *pol* gene also influence neurovirulence (9). However, our serial studies using chimeras from A8-V and 57 virus (57-V), the

*Address correspondence to Dr. Rihito Watanabe, Department of Bioinformatics, Faculty of Engineering, Soka University, Tangi-cho 1–236, Hachioji, Tokyo 192–8577, Japan. Fax: +81–426–91–9465. E-mail: rihito@t.soka.ac.jp

Abbreviations: A8-V, A8 virus; CNS, central nervous system; DAB, 3,3'-diaminobenzidine tetrahydrochloride; EcoR, receptor proteins for ecotropic retroviruses; Env, envelope protein (gp70); 57-V, 57 virus; FrC6-V, FrC6 virus; Fr-MLV, Friend murine leukemia virus; HE, haematoxylin and eosin; MEM, minimum essential medium; NRK, normal rat kidney; PAP, peroxidase-anti-peroxidase; PBS, phosphate-buffered saline; PFU, plaque forming unit.

latter of which is a non-neuropathogenic strain of Fr-MLV proved that the *gag* gene does not need to originate in a neuropathogenic virus in order for a virus to cause neurological disease (16). As part of these studies, we developed recombinant viruses R7c and R7f which lack the enhancer element found in A8-V after the replacement of the fragment with the enhancer element derived from the 57-V gene. These recombinant viruses induced spongiosis with a high incidence, although the isolated viral titers of the infected brain were very low. The mechanism by which viruses with low titers following CNS infection can induce distinct neuropathological lesions was partially revealed by immuno-histochemical studies (21) in which the expression levels of viral antigens following infection with A8-V, R7c, R7f or non-neuropathogenic recombinant virus Rec5 were studied. We employed specific antibodies raised against Env and Gag proteins to evaluate viral antigen expression in blood vessel walls and glia cells in infected brains using the criteria provided in our scoring system. Our data showed that the expression scores of the R7c and R7f viruses were comparable to those of A8-V but distinctly higher than those of Rec5, the latter of which was only minimally expressed in the infected CNS (21).

In this paper, we have compared viral antigen expression levels and neuropathological severity following infection with the A8-V and the PVC211. The main target of A8-V and PVC211 is CNS vascular walls (4, 16), namely endothelial cells (7, 8). The viral antigens in the endothelial cells are distributed not only in or near to the spongiform lesions but also in the areas that appear normal (2, 21). In addition, the viral antigens are not expressed in the neurons of the infected animals although the vacuoles forming spongiosis are located in neuropils (15). The expression levels of Gag and Env proteins assessed after infection with A8-V are identical *in vivo* (21) and *in vitro* (19).

Materials and Methods

Viruses and inoculation. PVC211-producing normal rat kidney cells (NRK) were kindly provided by Dr. Kai (Yamaguchi University, Yamaguchi, Japan). Friend murine leukemia virus (Fr-MLV) clone A8-V was obtained from the virus FrC6-V as described previously (15). Viral titers were determined by the XC cell plaque assay using C182 cells (14) in the presence of 10 µg/ml of Polybrene (14). C182 cells were grown on minimum essential medium (MEM) supplemented with 10% calf serum.

The ability of the viruses to cause disease was assessed using newborn Lewis rats purchased from a

commercial breeder. Newborn rats were inoculated by intra-peritoneal (0.1 ml) and intra-cerebral (0.0005 ml) routes with viral supernatant ($1-30 \times 10^4$ XC-PFU/head). Infected animals were then exsanguinated under deep anesthesia and the dissected organs were homogenized in cold phosphate-buffered saline (PBS) containing 1 mM MgCl₂ and 1 mM CaCl₂. Infectious virus titers were then determined by the XC cell plaque assay (14).

Histology. Following exsanguination of the animals 6-7 weeks after infection, the collected organs were immersed and fixed in 4% paraformaldehyde buffered with 0.12 M phosphate (pH 7.3). Tissues were then embedded in paraffin for histological staining with haematoxylin and eosin (HE).

The degree of spongiform neurodegeneration was scored as follows: 0—no lesions; 1—less than 20 vacuoles in the total area; 2—20 to 100 vacuoles counted in the light microscopical field at 10× magnification (field (×10)); 3—clusters consisting of over 100 vacuoles spread within one field (×10); 4—more than two clusters consisting of over 100 vacuoles in the area, or clusters of vacuoles occupying over 30% of the total area. Intermediate scoring in between each of the seven established scores was permitted by adding a value of 0.5 to the lower score. To score CNS pathology, five areas were selected: cerebral cortex, thalamus, cerebellum, pons and spinal cord.

For detection of the viral antigen proteins Env and Gag, we performed immunohistochemistry using goat anti-Rauscher MLV gp70 (antiEnv) (Quality Biotech Incorporated Resource Laboratory) and anti-AKR p30^{Gag} (antiGag, Quality Biotech Incorporated Resource Laboratory) on thin paraffin sections (2). Non-specific antibody binding was blocked by incubation of sections and cells with 50% normal mixed serum (fetal calf, calf, pig, and horse) diluted in PBS. Biotinylated rabbit anti-goat IgG (ZYMED Laboratories, Inc.) was used as a secondary antibody followed by treatment with an avidin-peroxidase complex (ZYMED Laboratories, Inc.). Washes in PBS were carried out between each step. After primary antibody incubation, the non-specific activity of endogenous peroxidase activity was blocked by incubating cells with 0.3% H₂O₂ in methanol. For the peroxidase reaction, 0.2 mg/ml 3,3'-diaminobenzidine tetrahydrochloride (DAB) (DOTIDE) in 0.1 M Tris buffer (pH 7.6) was used. In order to confirm that most of the glial cells carrying viral antigens are microglia, double immunostaining was carried. ED-1 monoclonal antibody was used to detect microglia as primary antibody (22). The antiGag reaction was developed first using the PAP method and donkey anti-goat IgG (Bethyl Lab., Inc.), peroxidase labeled goat IgG (DACO), and DAB, to yield a brown

reaction product. ED-1 was visualized using 20 mg/ml of 4-chloro-1-naphthol (WAKO, Japan), which gave a purple reaction product after sequential application of biotinylated rabbit anti-mouse antibody (ZYMED Laboratories, Inc.) and an avidin-peroxidase complex (ZYMED Laboratories, Inc.). Nuclei were counterstained with methyl green.

The intensities of antigen expression were scored separately either in blood vessels or in glial cells of the CNS. Scoring was performed in the same areas used for pathological evaluation. The degree of antigen expression in the blood vessels was scored as follows: 0—no antigens; 1—less than 10% of antigen-positive blood vessels in the sample area; 2—10–20% antigen-positive blood vessels in the sample area; 3—20–50% antigen-positive blood vessels in the sample area; 4—more than 70% antigen-positive blood vessels in the sample area. The degree of antigen expression in glial cells was scored as follows: 1—a few antigen-positive glial cells in total area; 2—more than 10 antigen-positive glial cells in the field at 10 \times magnification (field (\times 10)); 3—more than three fields (\times 10) that contain more than 10 antigen-positive glial cells; 4—fields with more than 10 antigen-positive glial cells occupy more than 70% of the area.

Results

Clinical Sign

None of the 10 rats that were infected with A8-V developed hind-leg paralysis or weakness within 6 weeks after inoculation and three out of ten infected rats manifested hind-leg paralysis afterwards. Three rats infected with A8-V did not show any neurological signs over the course of 8 weeks post inoculation. In contrast, half of the PVC211 infected rats developed hind-leg weakness within 6 weeks of inoculation and most (11/12 infected rats) manifested hind-leg paralysis by 8 weeks post inoculation.

Virus Growth

The virus titers recovered from the brains and spinal cords 6–7 weeks after infection with the A8-V ranged 3–50 \times 10⁴ and 9–60 \times 10⁴, respectively. The averages obtained from five infected rats were 1.8 \times 10⁵ and 3.4 \times 10⁵ respectively (Fig. 1). The infection of the PVC211 induced similar level of viral recovery from the brain and the spinal cord at 6–7 weeks post inoculation ranging from 1.3–3.7 \times 10⁴ and 4.8–7.2 \times 10⁴, respectively. The averages obtained from four rats infected with PVC211 were 3.0 \times 10⁴ and 6.1 \times 10⁴ respectively.

Histopathology

The degree of spongiotic change induced by the infection was assessed by a scoring system (see "Materials and Methods") after evaluation of 5 areas (cerebral cortex, thalamus, cerebellum, pons, and spinal cord) of each infected animal. A typical spongiosis scored as 3 is shown in Fig. 2. There, the HE staining illustrates many vacuoles with diameters of 5–100 μ m compose a fairly well demarcated area of spongiosis (Fig. 2A). The average scores obtained from the spinal cords of 7 rats infected with the A8-V and 3 rats infected with PVC211 were 1.4 and 2.8, respectively (Fig. 1), suggesting that PVC211 induced more severe neuropathology in the spinal cord compared to A8-V ($P < 0.002$ by Student's test). The average neuropathological scores in the cerebral cortex, thalamus, pons, and cerebellum (designated cumulatively as Brain in Fig. 1) were similar in PVC211 and A8-V infected rats ($P > 0.7$).

Histochemistry

Viral antigens were detected predominantly in the vascular walls of infected brains regardless of the virus used (Fig. 2E), and with the exception of the vascular wall, were detected at lower frequencies in glial cell structures (Fig. 2, C and F). The glial structures associated with viral antigens were regularly encountered close to and inside spongiotic lesions and were often attached to the wall of the vacuole (Fig. 2C). On the other hand, virus-expressing blood vessels exhibited a much wider distribution, and were often found in the regions where no spongiosis was observed (Fig. 2E).

This closer correlation of antigen expression to the lesions in glial cells than in vascular walls was statistically analyzed. The expression levels of the Env protein were evaluated according to our evaluation score (see "Materials and Methods"), examined in selected five areas within the CNS as described earlier for a pathological scoring system. When the expression levels of the viral antigen in the glial cells (env/glia in Fig. 1) activated in the spinal cords were compared between PVC211 and A8-V infection, PVC211 infection induced more than twice the levels of antigen expression in glial cells compared to A8-V ($P < 0.04$). In contrast, no significant difference was observed in the expression of Env protein in the vascular walls following infection by these viruses (env/vessel in Fig. 1) in the spinal cord ($P > 0.3$). Furthermore, there also was no significant difference in the env/glia immunohistochemical scores obtained from the brain (cerebral cortex, thalamus, pons, and cerebellum, designated as Brain in Fig. 1) between the PVC211 and A8-V infected groups ($P > 0.4$).

In order to confirm the previous report that spongi-

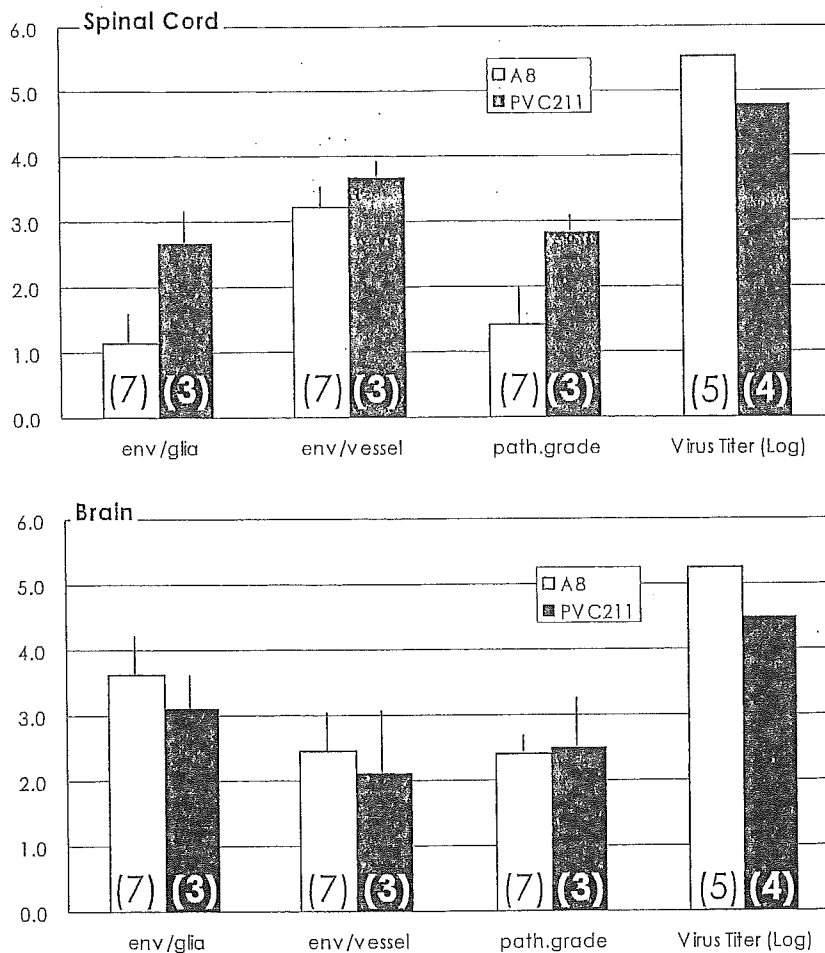


Fig. 1. Histological scores and viral growth. Numbers in the parentheses described in the bars indicate the numbers of rats examined. Env expression estimated by immuno-histochemistry either in the blood vessel wall or glia cells is described as Env/vessel or glia, respectively, and the pathological grade as path. grade. The immunohistochemical and pathological scores of each animal was evaluated by the averaging the data obtained from spinal cord or brain which is investigated in 4 different areas (cerebral cortex, thalamus, cerebellum, and pons).

form degenerations induced by several neuropathogenic murine retroviruses are associated primarily with infection of microglial cells (13), we performed double immunostaining. Our data showed that many of the glial cells that bore viral antigen (Fig. 2F) also expressed a microglial marker protein that was identified by the monoclonal antibody ED-1 (Fig. 2F).

Discussion

Our data showed that PVC211 was more neuropathogenic in neonatal rats than A8-V, as manifested by the higher incidence and more rapid onset of hind-leg paralysis in these animals. This neurological sign was due to the presence of pathological lesions in the spinal cord, which have also been investigated in other neurological diseases which are experimentally induced in rats, such as experimental allergic encephalomyelitis

(2). Our neuropathological data confirmed the presence of viral lesions in the spinal cord of rats that developed paralysis and, as expected based on our neurological findings, rats that were infected with PVC211 showed more of such lesions.

The above data notwithstanding, viral titers recovered from the spinal cords of PVC211 and A8-V infected rats were similar (Fig. 1). From a virological view point, it has been considered that the level of viral titer obtained from a target organ is correlated to pathological severity in the relevant organs (11, 13, 14). However, our recent studies using chimeric viruses derived from the genes of A8-V and a non-neuropathogenic Fr-MLV, 57-V revealed that neuropathology induced by A8-V infection is not dependent upon the viral proliferation rate but rather the level of viral antigen expression (19). Nevertheless, this comparative study using chimeras resulted in a comparison between neuropathogenic and

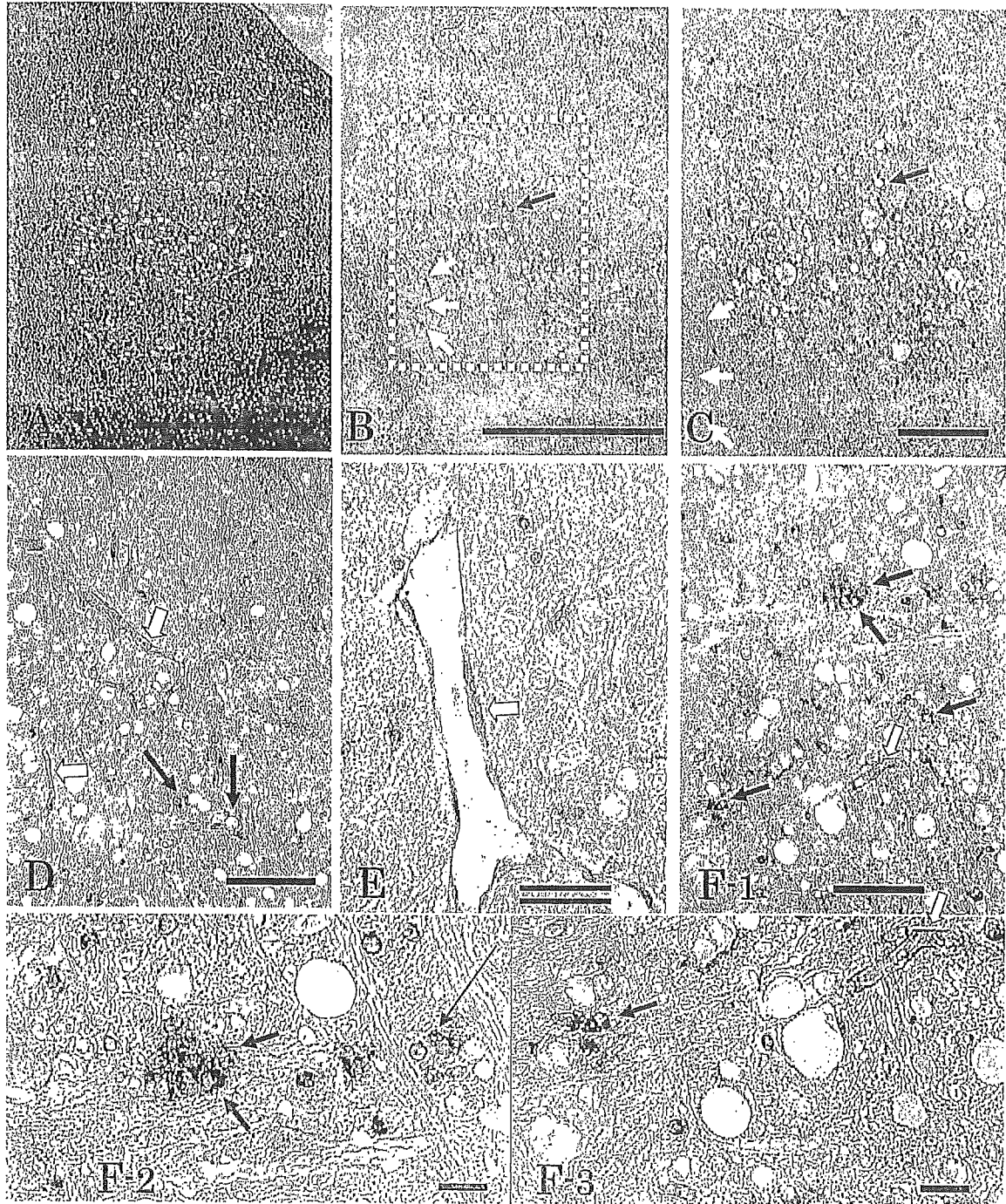


Fig. 2. Histology after infection. HE staining (A) and immuno-histochemistry (B-E) using anti-Gag or anti-Env protein antibodies (designated as Gag or Env in each photograph respectively) 8 weeks after infection with A8-V or PVC211. The inoculated virus is indicated in each photograph. A-D: Areas around the lateral cerebellar nucleus stained for serial sections. The black arrows indicate glial cells bearing viral antigen which attach to the vacuolar wall while the white arrows indicate the antigen-positive blood vessels. The rectangular region in figure B is shown at higher magnification in C. The expression levels of Env (C) and Gag proteins (D) were similar as we previously reported (in press). E: Note the antigen-positive blood vessel indicated by the white arrow in the area of normal appearance. F: Double immunostaining for Gag protein (brown color) and a microglial marker protein (purple color). Pictures taken at higher magnification of F-1 are shown in F-2 and F-3. Note the viral antigen-positive blood vessel (brown staining) at the white arrow and the double labeled microglial cells staining brown and purple at the bolded black arrows. The long black arrow indicates a positively stained (purple) uninfected microglial cell. The single bars and double lines indicate 500 μm and 125 μm , respectively.

non-neuropathogenic chimerae, and the viral antigen expression in blood vessel walls of the CNS infected with non-neuropathogenic chimerae was also suppressed as well as in glial cells (19). Therefore, the significance of viral antigen positive glial cells in forming spongiotic lesions could not be evaluated in the comparative study mentioned above.

We have proposed that glial cells carrying viral antigens might contribute to developing neuropathological lesions induced by A8-V infection, because we often observe the antigen positive glial cells attaching to the walls of vacuoles which compose spongiotic lesions (17, 21). In addition, numerous reports have suggested that spongiform degeneration induced by neuropathogenic murine retroviruses is primarily associated with infection of microglial cells (1, 3, 6, 12). The results of our double labeling study confirmed that A8-V infection also induces many microglial cells which carry viral antigens (Fig. 2F). However, the importance of the suggested association of infected microglia with neuropathological lesions remains unknown, because viral antigen positive blood vessel walls are encountered in much higher frequency than viral antigen positive microglia in infected CNS (4, 7, 17, 20), and no statistical analysis had been done until now. In this paper, we clarified that viral antigen positive microglial cells were really associated with lesional distribution after a statistical analysis. Furthermore, distribution of antigen positive blood vessels was proved not to be statistically correlated with that of neuropathological lesions. Neuropathological changes induced by infections of A8-V and PVC211, which share a common genetical background, were almost identical except for the intensity of lesions in spinal cords, where similar levels of viral antigen expression in blood vessel walls were obtained from those viral infections. It is not clear how PVC211 induced a higher population of infected microglial cells in infected spinal cords than A8-V, in spite of the fact that these two viruses exhibit similar viral titers in brains and in spinal cords as well. The difference in the infectivity of the two viruses to glial cells in spinal cords might be due to different proliferation rates of these viruses during an earlier period of infection than the time when we compared the outcome at 6–8 weeks after infection, because the viral titers recovered from the CNS infected with A8-V at the newborn stage reach a plateau at 3–4 weeks after infection (15). And the expression levels of the receptor proteins for ecotropic retroviruses (EcoR) in rat brains change at the age of 4–5 weeks (17). We molecularly cloned the EcoR gene from F10 cells (F10-EcoR) (16), which are derived from rat glial cells. Application of a specific antibody for F10-EcoR protein visualized, by an immunohisto-

chemical procedure, the F10-EcoR protein expression both in blood vessel walls and in glial cells of the CNS (16). The expression level of the F10-EcoR protein in rat glial cells reduced dramatically at the age of 4 weeks old, while that in the blood vessel walls of the rat CNS was well maintained afterwards (17). Although a close association of viral antigen positive microglial cell with lesional distribution was indicated, we still do not have any evidence or information as to whether those antigen positive microglial cells really create the vacuoles in the neuropils.

The authors thank Katsumi Goto for performing the histological studies. This work was supported in part by a Grant-in-Aid for Scientific Research from the Japan Society for the Promotion of Science and "High-Tech Research Center" Project for Private Universities: matching fund subsidy from MEXT, 2004–2008.

References

- 1) Baszler, T.V., and Zachary, J.F. 1991. Murine retroviral neurovirulence correlates with an enhanced ability of virus to infect selectively, replicate in, and activate resident microglial cells. *Am. J. Pathol.* **138**: 655–671.
- 2) Fukumitsu, H., Takase-Yoden, S., and Watanabe, R. 2002. Neuro-pathology of experimental autoimmune encephalomyelitis modified by retroviral infection. *Neuropathology* **22**: 280–289.
- 3) Gravel, C.D., Kay, G., and Jolicœur, P. 1993. Identification of the infected target cell type in spongiform myeloencephalopathy induced by the neurotropic Cas-Br-E murine leukemia virus. *J. Virol.* **67**: 6648–6658.
- 4) Ikeda, T., Takase-Yoden, S., and Watanabe, R. 1995. Characterization of monoclonal antibodies recognizing neurotropic Friend murine leukemia virus. *Virus Res.* **38**: 297–304.
- 5) Kai, K., and Furuta, T. 1984. Isolation of paralysis-inducing murine leukemia viruses from Friend virus passaged in rats. *J. Virol.* **50**: 970–973.
- 6) Lynch, W.P., Robertson, S.J., and Portis, J.L. 1995. Induction of focal spongiform neurodegeneration in developmentally restricted mice by implantation of murine retrovirus-infected microglia. *J. Virol.* **69**: 1408–1419.
- 7) Masuda, M., Hanson, C.A., Dugger, N.V. et al. 1997. Capillary endothelial cell tropism of PVC-211 murine leukemia virus and its application for gene transduction. *J. Virol.* **71**: 6168–6173.
- 8) Masuda, M., Kakushima, N., Wilt, S.G. et al. 1999. Analysis of receptor usage by ecotropic murine retroviruses, using green fluorescent protein-tagged cationic amino acid transporters. *J. Virol.* **73**: 8623–8629.
- 9) Masuda, M., Remington, M.P., Hoffman, P.M., and Ruscetti, S.K. 1992. Molecular characterization of a neuropathogenic and nonerythroleukemogenic variant of Friend murine leukemia virus PVC-211. *J. Virol.* **66**: 2798–2806.
- 10) Odaka, T., Ikeda, H., Yoshikura, H., Moriwaki, K., and